ELSEVIER

Fractal Modeling of Airborne Laser Altimetry Data

Yakov A. Pachepsky,[*1] *Jerry C. Ritchie,*[†] *and Daniel Gimenez*[†]

Airborne laser altimetry is a remote sensing technique that can provide high resolution data on the roughness of the landscape both for estimating water balance components and for distinguishing between landscapes. Models of the scale-dependent roughness are needed to find scales most appropriate for these purposes. Our objectives were to apply fractal scaling to high-resolution profiling laser altimetry data and to determine fractal parameters for differentiating land cover. Data were collected at the USDA-ARS Jornada Experimental Range in New Mexico over grass-dominated and shrub-dominated sites along four transects at each site. Scale-dependent root-mean-square (RMS) roughness and data power spectrums were computed from 100,000 data points (~2 km) from each transect. A linearity measure and piecewise linear approximation were applied to find intervals of the fractal scaling. The RMS roughness data had two intervals of self-affine fractal scaling on grass transects and four such intervals on shrub transects. Reduction in the number of data points did not lead to a decrease in roughness but caused a smoothing dependency of fractal dimension on scale. Ten- and hundred-meter scales were appropriate for distinguishing between grass and shrub transects on the basis of fractal dimensions. Published by Elsevier Science Inc.

*USDA ARS Remote Sensing and Modeling Laboratory, Beltsville, MD USA

†USDA ARS Hydrology Laboratory, Beltsville, MD USA

[1]Yakov A. Pachepsky works for the Duke University Phytotron, Duke University, Durham, NC 27706, through a specific cooperative agreement with the USDA ARS Remote Sensing and Modeling Laboratory

Address correspondence to Dr. Yakov A. Pachepsky, USDA ARS Remote Sensing and Modeling Laboratory, BARC-West, Bldg. 7, Room 8, Beltsville, MD 20705.

Received 21 May 1996; revised 26 November 1996.

INTRODUCTION

Airborne laser altimetry is a remote sensing technique that can provide high vertical and horizontal resolution data (Ritchie, 1995). Such high-resolution measurements provide detailed data on the roughness of the landscape, which is a key property in assessing components of the evapotranspiration demand (Menenti and Ritchie, 1994). In particular, aerodynamic roughness can be estimated from data on landscape roughness. Land cover and landforms affect roughness, and roughness can be used to distinguish between landscapes. Models of dependencies of roughness on scale are needed to use laser altimetry data for this purpose.

Fractal geometry provides appropriate tools to quantify scale-dependent roughness. Fractal models are designed to describe rugged surfaces displaying a similarity in features persisting over a range of spatial scales. This kind of similarity has been observed for the topography of the Earth's surface obtained from digitized maps (Klinkenberg and Goodchild, 1992; Mark and Aronson, 1984; Ouchi and Matsushita, 1992) and for sonar measurements of seabeds (Fox and Hayes, 1985; Gilbert, 1989; Malinverno, 1989). For fractal scaling, remote sensing images can be considered a topographical surface (De Jong and Burrough, 1995). Fractal modeling has been applied to ground-based photography (Carr, 1990), aeromagnetic data (Gregotsky et al., 1991), Landsat thematic mapper images (DeCola, 1989; Lam, 1990), thermal infrared multispectral data (Jaggi et al., 1993), and airborne imaging spectrometer data (De Jong and Burrough, 1995).

Fractal geometry was developed to describe the hierarchy of ever-finer details in the real world. Natural objects have similar features at various scales. Measures of these features (e.g., the total number of features, the total lengths, the total mass, the average roughness, the total surface area, etc.) are dependent on the scale at which features are observed. This dependence is the

REMOTE SENS. ENVIRON. 61:150–161 (1997)
Published by Elsevier Science Inc.
655 Avenue of the Americas, New York, NY 10010

0034-4257/97/$17.00
PII S0034-4257(96)00249-0

same over a range of scales (i.e., scale invariant within this range). When expressed mathematically, the dependence becomes a fractal scaling law. In a classic example, "the length of the coastline increases as the length of the measuring rod decreases according to a power law. The power determines the fractal dimension of the coastline" (Turcotte, 1992). The larger the fractal dimension, the more rugged is the object under study.

Both isotropic and anisotropic fractals are found in topography (Turcotte, 1992). Self-similar fractals are isotropic, which means that, in two-dimensional x-y space, $f(x,y)$ is statistically similar to $f(rx,ry)$, where r is a scaling factor. Self-affine fractals are anisotropic, which means that, in two-dimensional x-y space, $f(x,y)$ is statistically similar to $f(rx,r^H y)$, where r is a scaling factor and H is called the Hurst exponent. That is, magnifying the horizontal scale r times has to correspond to magnifying the vertical scale r^H times (Mandelbrot, 1986). Surface measurements obtained by remote sensing or created from remote sensing data are usually treated as self-affine surfaces (Andrle and Abrahams, 1990; Polidori et al., 1991; Shepard et al., 1995) with different vertical and lateral scaling.

High values of the Hurst exponent indicate some memory or autocorrelation in the data. Low values suggest an anticorrelation or self-correcting response (Russ, 1994). The Hurst exponent is related to the fractal dimension D_s of the surface as (Mandelbrot, 1986)

$$D_s = 3 - H. \quad (1)$$

Smooth surfaces have fractal dimensions close to 2. Highly irregular surfaces have fractal dimensions close to 3.

A line formed as a cross section of any fractal self-affine surface and a vertical plane will also display self-affine properties. This line will have a fractal dimension D_L related to the fractal dimension of the surface and to the Hurst exponent H as (Mandelbrot, 1986)

$$D_L = D_s - 1 = 2 - H. \quad (2)$$

At any particular scale, any two consecutive height variations are likely to have opposite signs when the fractal dimension D_L is larger than 1.5. When the fractal dimension D_L is less than 1.5, any two consecutive height variations are likely to have the same sign (Polidori et al., 1991).

Fractal scaling is valid for a range of scales. Outside this range, the scaling may not be applicable at all or may be applicable with different fractal dimensions. In most studies in geomorphology and remote sensing, the total range of scales studied has encompassed two or more ranges of scales with distinctly different fractal dimensions (Andrle and Abrahams, 1990; Fox and Hayes, 1985; Hallet, 1989; Klinkenberg and Goodchild, 1992; Malinverno, 1989; Mark and Aronson, 1984).

Both the fractal dimension and boundaries of a fractal scale range are parameters of a fractal model (Pfeifer and Obert, 1990) and as such can be used to distinguish between surfaces or between cross sections of surfaces. Several authors have shown relations between landscape features and parameters of fractal models developed from topographic and remote sensing data (De Jong and Burrough, 1995; Klinkenberg and Goodchild, 1992; Mark and Aronson, 1984; Ouchi and Matsushita, 1992).

Several methods have been proposed to estimate fractal dimensions from measurements of self-affine surfaces. Different methods usually yield different results (Klinkenberg and Goodchild, 1992; Shepard et al., 1995). Sometimes the differences are explained by the fact that, even if the surface or line is an ideal fractal, the discrete sampling, resampling, and filtering of data may cause a loss of information (Dubuc et al., 1989; Malinverno, 1990). Another explanation assumes that the surfaces or lines under study are not ideal fractals, and this affects the results of different methods in different ways (Jaggi et al., 1993; Roach and Fouler, 1993). Methods may vary in their sensitivity to noise in the data (De Jong and Burrough, 1995). Boundaries of the range where the self-affinity holds are often found manually. This may serve as an additional source of uncertainty (Rees and Miller, 1990; Yokoya et al., 1989).

Even if the same method of data analysis is used, values of the fractal parameters may depend on the noise and the pixel size inherent to remote sensing technique used to measure the variable of interest (De Jong and Burrough, 1995).

The USDA ARS Jornada Experimental Range has a long-term experimental program designed to study changes in vegetation pattern and to estimate water balance of desert ecosystems. The laser altimetry data collected at this site are being used to estimate the aerodynamic roughness and to measure vegetation properties. The objectives of this study were to use laser altimeter data to determine fractal properties of the landscape surface roughness at different scales and to use fractal properties to discriminate landscapes with different land covers.

MATERIALS AND METHODS

Study Area

Airborne laser altimetry data were collected at the USDA ARS Jornada Experimental Range in southern New Mexico. The Jornada Experimental Range lies within the Chihuahuan Desert ecosystem. Annual averages for precipitation and temperature are 241 mm and 15°C, respectively. Flora is characteristic of a subtropical ecosystem in the hot desert biome. Grasses and shrubs dominate the area landscapes.

The Experimental Range is located on the La Mesa geomorphic surface of middle Pleistocene age (>400,000 B.P.). The ancestral Rio Grande river deposited sediments on this plain. The study sites have Typic Haplar-

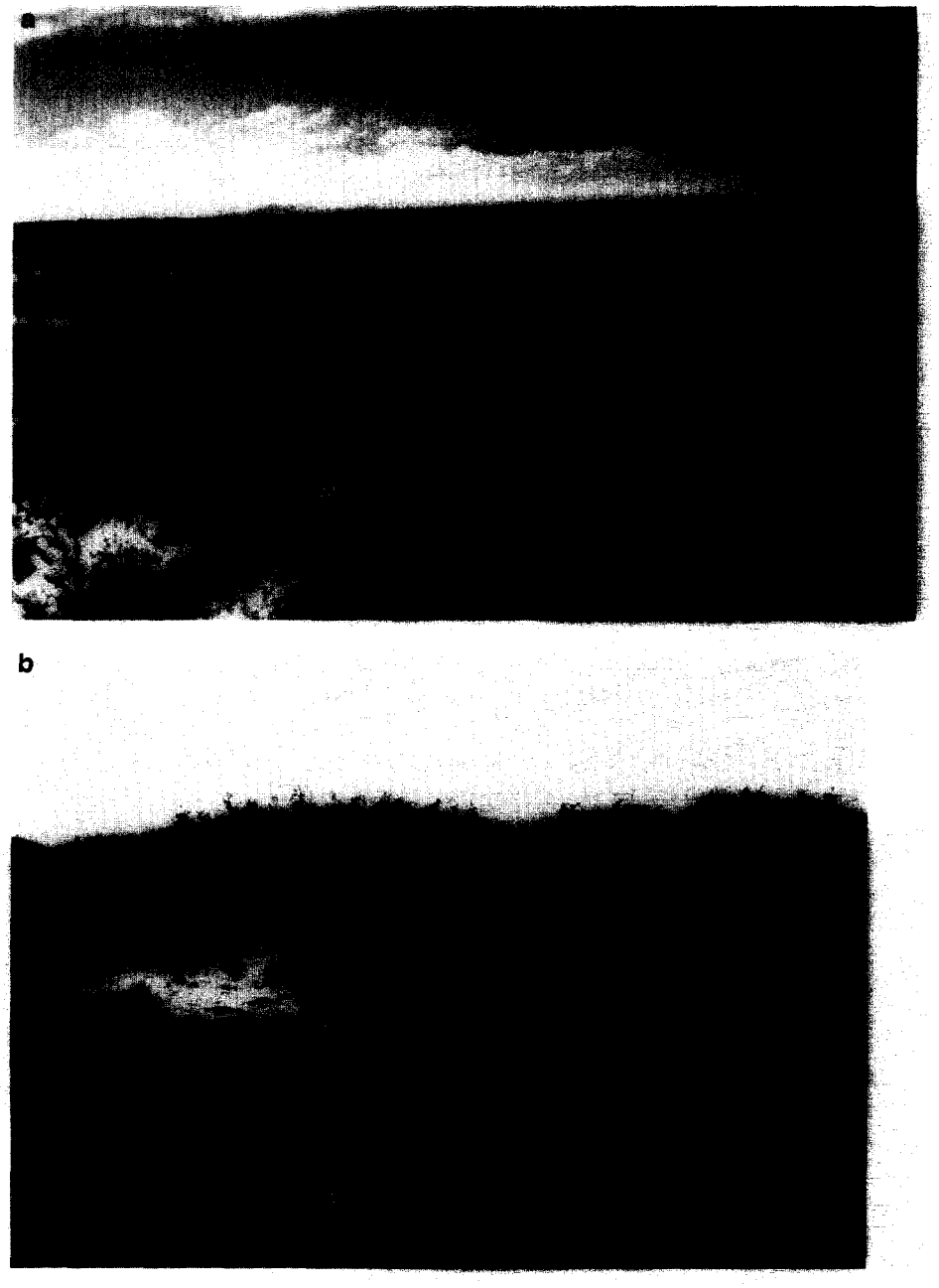

Figure 1. Typical views of grass-dominated (a) and shrub-dominated (b) landscapes in the USDA-ARS Jornada Experimental Range.

gid and Paleargid soils that have developed from alluvium in level basins below the piedmonts. Wind in this region commonly modifies these gentle sloping surfaces. The soils are loamy sands and fine loamy sands typical of the Onite, Pajarito, Pintura, and Wink series. These soils are moderately deep but have calcic horizons of varying thicknesses relatively close to the surface. Detailed description of relief and vegetation patterns can be found in the paper by Buffington and Herbel (1965).

Laser altimetry data collected over grass-dominated and shrub-dominated sites were used in the analyses. Typical views of the two types of landscape are shown in photographs in Fig. 1. The grass site had a uniform cover of black grama on level ground with only small undulations. Honey mesquite on coppice dunes dominated the shrub site (Buffington and Herbel, 1965). The dominant wind direction is from the southwest, coppice dunes tend to be oval rather than circular, with their longest diameter in the southwest to northeast direction. These coppice dunes range in height from 2 to 8 m and in diameter from 3 to 15 m.

Laser Measurements

A laser altimeter mounted in an airplane was used to measure the distance from the airplane to the landscape surface. The altimeter is a pulsed gallium-arsenide diode laser, transmitting and receiving 4000 pulses/s at a wavelength of 904 nm. The field of view of the laser is 0.6

mrad, which gives a "footprint" on the ground that is approximately 0.06% of the altitude. The timing electronics of the laser receiver allow a vertical resolution of 5 cm for each measurement.

Digital data (distance from the airplane to the landscape surface) from the laser receiver along with data from a gyroscope and an accelerometer mounted on the base of the laser platform are recorded with a portable personal computer. A video camera, borehole sighted with the laser, records an image of the flight line. Sixty video frames are recorded per second, and frames are annotated with consecutive numbers, clock times, and ground-positioning-system data. Each video frame number is recorded with digital laser data by the computer to allow precise correlation of the laser data on the landscape with the video data for these studies.

Four airborne laser transects, referred to as A, B, C, D, were made at the grass site and four (E, F, G, H) were made at the shrub site in May 1995. At each site, two transects were in the north-south (C, D, G, H) direction and two were in the east-west (A, B, E, F) directions, all from an altitude of 200 m. The data sets used in the fractal analyses included 100,000 laser measurements (approximately 2 km) for each of the eight laser transects. The total number of transects reflected resources available for this study.

Landscape surface elevation was calculated for each laser measurement by using known ground elevations along a flight line to convert the relative data into absolute elevations.

Data Analysis

Construction of a fractal model for a line includes the (1) selection of a property to be calculated on different scales, (2) selection of a procedure to define ranges of scales within which the self-affinity exists, and (3) selection of a method to calculate fractal dimensions for each range of the self-affinity.

We calculated the root-mean-square roughness known to display fractal scaling along the cross sections of self-affine surfaces (Russ, 1994). Root-mean-square roughness is the root-mean-square (RMS) value of residuals on a linear trend fitted to the sampled points in an interval (Malinverno, 1990). The interval is called a "window." The RMS roughness is found as

$$\mathrm{RMS}(w)=\frac{1}{n_w}\sum_{i=1}^{n_w}\sqrt{\frac{1}{m_i-2}\sum_{j\in w_i}z_j^2}, \tag{3}$$

where n_w is the total number of windows of length w, m_i is the number of points in the window, and z_j are residuals of the trend. Following the recommendations of Malinverno (1990), we began with a short span containing at least 10 points and increased to window lengths that were 20% of the total length of the data series, and we made adjacent windows overlap by 50% of the window length. The window length was incremented by one sampling interval Δx; that is, each window of a new scale covered one extra point in comparison with the preceeding scale. In the range of scales, where the dependence of log(RMS) on log(w) is linear, the slope of this dependence is the Hurst exponent H introduced in Eqs. (1) and (2).

For the purpose of using fractal parameters to discriminate between landscapes, we calculated the power spectrum of the elevation data along transects. The spectral method is the most widely used (Turcotte, 1992) and is based on the inference that a self-affine series should have a power spectrum

$$P(f)=Cf^{-\beta}, \tag{4}$$

where P is power (i.e., mean square amplitude), f is frequency, C is a scaling coefficient, and the spectral exponent β is related to the fractal dimension by

$$D_L=\frac{5-\beta}{2}. \tag{5}$$

We plotted log(P) versus log(T), where $T=\Delta x/f$ is the wavelength of harmonic oscillations. In the range of scales, where the dependence of log(P) on log(T) is linear, the slope of this dependence is equal to β introduced in Eqs. (4) and (5).

To define ranges of scales over which self-affinity exists, we tested two procedures: the calculations of (1) a linearity measure and (2) a piecewise linear approximation. The linearity measure L introduced in fractal modeling by Yokoya et al. (1989) and Rees and Miller (1990) is calculated for the set of points in a plane as

$$L=\frac{\sqrt{4\sigma_{xy}^2+(\sigma_{yy}-\sigma_{xx})^2}}{\sigma_{yy}+\sigma_{xx}}, \tag{6}$$

where σ_{xx}, σ_{yy}, and σ_{xy} represent the variance of x-coordinates, the variance of y-coordinates, and the covariance between x and y coordinate sets, respectively. This measure L falls between 0 and 1, being equal to 1 for points on a straight line and equal to 0 for uncorrelated randomly distributed points. To separate linearity intervals on log-log plots, the value of L is computed for the first four points, then for the first five points, and so on, while the value of L increases. The end of the first linearity interval will be in the point after which the value of L begins to decrease. Then the next point is considered the first point of the next linearity interval. This point is used as the first one in computations of L for the expanding sets of points while L increases. The end of the second linearity interval will again be in the point after which values of L begin to decrease. Then the next point is considered the first point of the third linearity interval, and so forth. The separation of linearity intervals ends when all points are used in computations. For each linearity interval, a linear regression over points within this interval yields the value of H or the value of β if the

dependencies of log(RMS) on log(w) or dependencies of log(P) on log(T) are analyzed, respectively. The fractal dimension of the line D_L is obtained from Eq. (2) or (5).

To do the piecewise linear approximation of data on log-log plots, we inspected the plots and selected the total number of linear segments by visual check. Then we applied the technique described by Pachepsky et al. (1995). A piecewise linear approximation of the dependence of ln(RMS) on ln(w) has been used in the form

$$\ln(\mathrm{RMS})^{\mathrm{calc}}=B+\sum_{j=0}^{L-1}(D_{j+1}-D_j)\ln(w_j)+(2-D_L)\ln(w),\ w_j\leq w<w_{j+1},\quad L=1,2,\ldots,M \tag{7}$$

Here M is the assumed number of linearity intervals in the structure; $w_0, w_1, \ldots, w_M$ are cutoffs of the sequential fractal intervals; w_{j-1} and w_j are lower and upper cutoffs of the jth linearity interval; D_j is the fractal dimension at the jth interval; B is a matching constant; and $D_0=D_1$. For example, a structure with three linearity intervals ($M=3$) is described by the formula

$$\ln(\mathrm{RMS})_i^{\mathrm{calc}}=\begin{cases}B+(2-D_1)\ln(w), & w_0\leq w<w_1\\ B+(D_1-D_2)\ln(w_1)+(2-D_2)\ln(w), & w_1\leq w<w_2\\ B+(D_1-D_2)\ln(w_1)+(D_2-D_3)\ln(w_2)+(2-D_3)\ln(w), & w_2\leq w\leq w_3\end{cases} \tag{8}$$

Average values of parameters B, $D_1, \ldots, D_m$, $w_1, \ldots, w_{M-1}$ have been estimated by nonlinear minimization of the lack-of-fit mean square, which is known to be an unbiased estimator of the model's standard error (Whitmore, 1991):

$$s_r=\sqrt{\frac{\sum_{i=1}^{N}m_i[\ln(\mathrm{RMS})_i^{\mathrm{calc}}-\ln(\mathrm{RMS})_i^{\mathrm{meas}}]^2}{N-P}}. \tag{9}$$

Here $(\mathrm{RMS})^{\mathrm{meas}}$ is the root-mean-square roughness estimated from measured values, $(\mathrm{RMS})^{\mathrm{calc}}$ is the root-mean-square roughness estimated from Eq. (2), N is the total number of measured RMS values, m_i is the number of replications in the measurements at the ith RMS value, and P is the number of parameters ($P=2M$ for this case). The Marquardt-Levenberg algorithm was used to estimate both the boundaries of the linearity ranges and the slopes of the segments approximating data within those ranges. Both values of parameters and standard errors of parameters were estimated in this way. To avoid local minima, we made 100 runs for each data set, each time randomly changing the initial estimates of all parameters.

Linearity intervals have to be wide enough to be considered ranges of the fractal scaling. The minimum theoretical ratio between upper and lower boundaries of the fractal scale range is $2^{1/D}$ (Pfeifer and Ober, 1990). A self-affine line may have this ratio between $2^{1/2}$ and 2. We excluded all linearity intervals for which the ratio of the boundaries was smaller than 2.

To compute Fourier spectra of data, we used standard programs (SPCTRM and FOUR1) developed by Press et al. (1990). The computer programs written in FORTRAN for all other computations are available upon request from the authors.

RESULTS

Plots of a typical laser altimetry profile of a north-south transect for the grass (Fig. 2) and shrub (Fig. 3) sites show the differences in surface properties at the sites. Figures 2 and 3 were plotted by using a 12-measurement block average to display the data and correspond to grass data transect C and shrub data transect G used in our analysis. The grass site shows a relatively smooth surface with an occasional shrub or taller object. The shrub site shows a topography of dunes superimposed on the relatively rough surface. Spikes correspond to shrubs.

Plots of the RMS roughness versus spatial scale are shown in Fig. 4. Visual inspection of graphs shows that more than one range of self-affine fractal scaling can be found and that different fractal dimensions can be expected in different ranges of scales. A difference was found between data for the grass and the shrub transects, using the RMS data (Fig. 4). Grass transects have low roughness with scales up to 20 m. At larger scales, the roughness steeply increases with scale and displays consistent fractal scaling. Shrub transects have the roughness rapidly increasing as the scale increases. At least four segments of linearity can be seen in the shrub-dominated transects.

The power spectrum plots (not shown) have more noise than the RMS roughness plots in Fig. 4. The differences between grass and shrub transects are still expressed. In grass transects, the amplitudes of the Fourier components with low wavelengths are small. Wavelengths T of 10–20 m mark the limit beyond which the power spectrum grows fast as T increases. The data show that more than two linearity intervals may be appropriate for grass transects. In shrub transects, the small wavelengths (1–5 m) correspond to larger power spectra than in the grass transects. At least four segments of linearity can be distinguished in the shrub transects.

Results of applying the linearity measure to separate different ranges of fractal scaling on roughness plots are shown in Figure 5. Grass transects have two or three linearity intervals within the 1–10 m scale range. The fractal dimension of those intervals is close to 2, inferring very high irregularity. Most of the differences between fractal dimension in these intervals are not statistically significant, but the linearity measure algorithm based on the linearity measure distinguishes between these intervals. The range of scales between 10 and 60 m includes 6–7 intervals of linearity, but all are too short to be considered true ranges of the fractal scaling. A large interval of fractal scaling lies between 60 and 200–300 m. Here

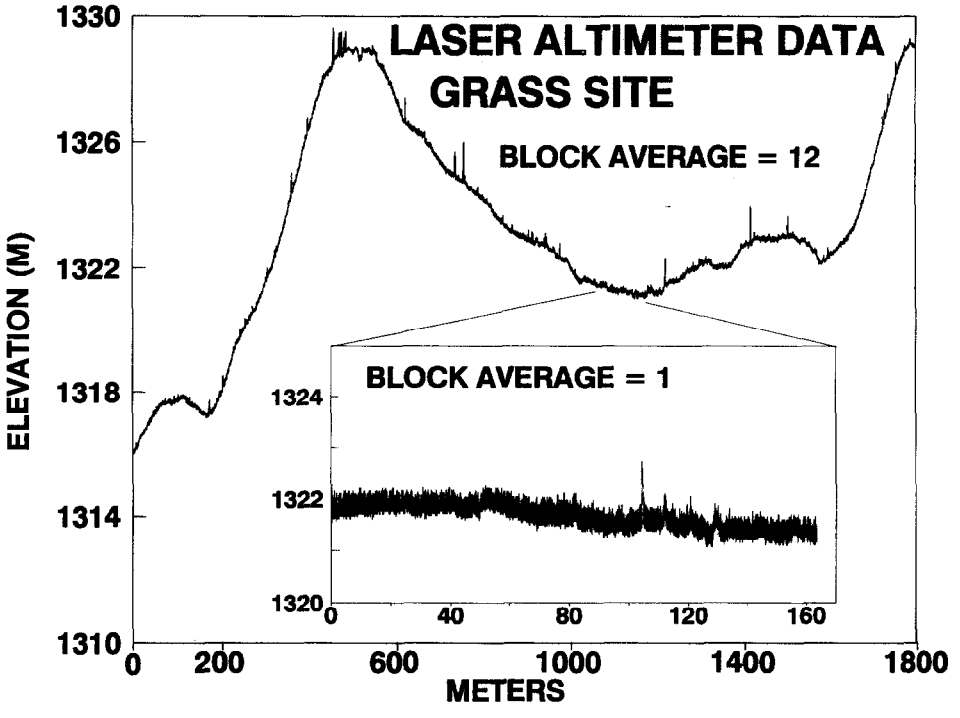

Figure 2. A laser altimetry profile of a north-south transect made at the grass-dominated site (C). Data were plotted by using a 12-measurement block average to display the data. Insert shows full-resolution laser data.

fractal dimensions are between 1.05 and 1.25 and correspond to low irregularity.

Shrub transects have three or four linearity intervals between 1 and 6 m (Fig. 5). Fractal dimensions are between 1.75 and 1.95 along these intervals and can be treated as intervals of fractal scaling. The range of scales between 6 and 15–30 m is the interval of fractal scaling where the transects show differences in fractal dimensions. The fractal dimensions are between 1.6 (east-west transects) and 1.75 (north-south transects), showing high irregularity. The next scaling range was found between 15–30 and 70–90 m. The irregularity is again high, with D_L between 1.7 and 1.8 for all transects. Finally, the range of largest scales, between 70–90 and 250–400 m,

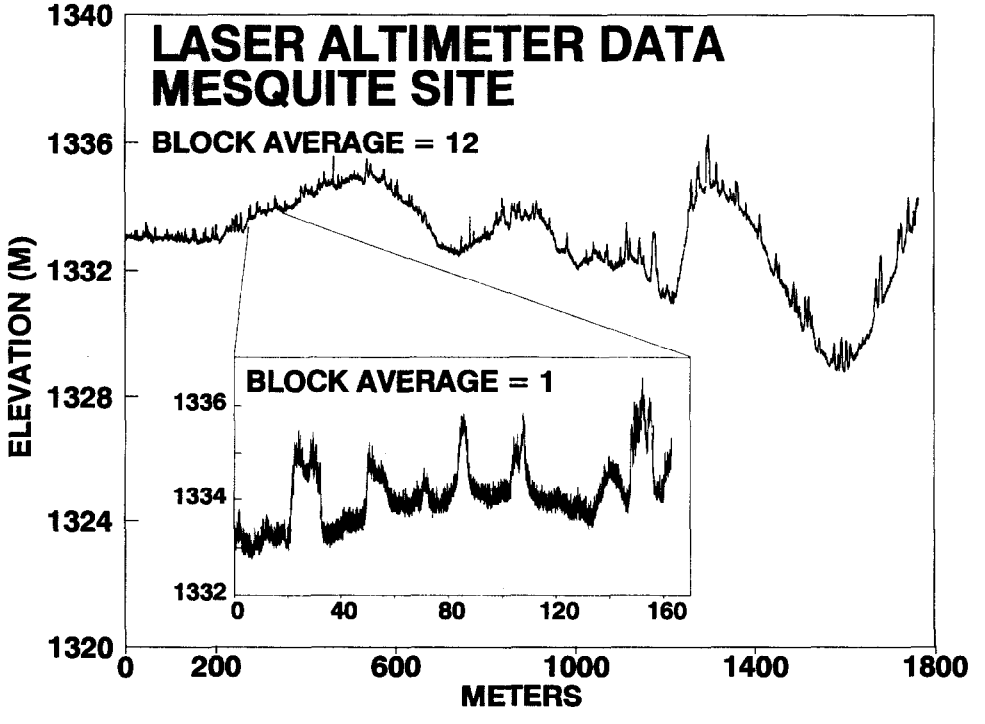

Figure 3. A laser altimetry profile of a north-south transect made at the shrub-dominated site (G). Data were plotted by using a 12-measurement block average to display the data. Insert shows full-resolution laser data.

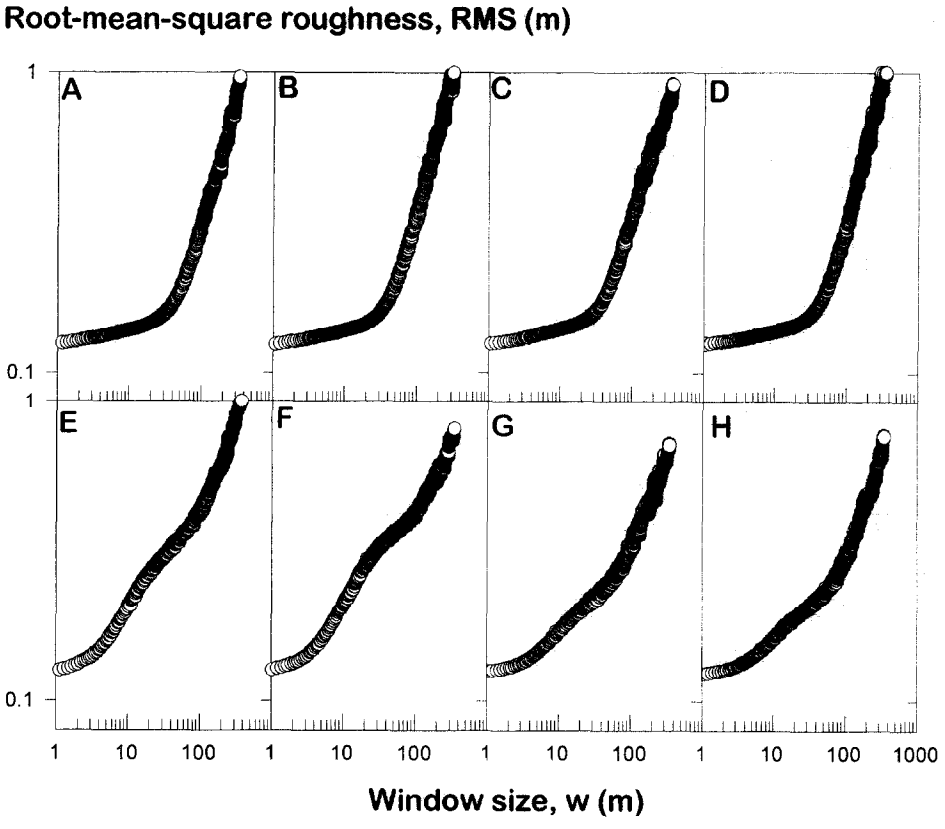

Figure 4. Log-log plots of root-mean-square roughness versus the length of intervals over which it was calculated (window size): (A–D) grass transects; (E–H) shrub transects.

has a moderate irregularity close to that of the white noise, with D_L about 1.5.

Because the grass and the shrub transects had different sequences of the fractal scaling intervals, a statistical comparison of within-landscape and between-landscape variation could be done where scaling ranges overlapped. Ten- and hundred-meter windows were appropriate for this purpose. In the scale ranges including 10-m windows, mean±standard deviation was 1.93±0.01 and 1.68±0.10 for the grass and shrub transects, respectively. In the scale ranges covering 100-m windows, mean±standard deviation was 1.15±0.10 and 1.45±0.08 for the grass and shrub transects, respectively. The difference between means in grass and shrub transects was significant at the 0.05 level both for 10-m and for 100-m windows as shown with two-sample heteroschedastic Student's test.

The piecewise linear approximation of roughness data in Figure 4 resulted in the estimates of fractal dimensions and scale range boundaries shown in Table 1. Estimated standard errors of all parameters are low (not shown), so the coefficients of variation are less than 2%. The piecewise linear approximation reveals qualitatively the same dependence of scaling as do the linearity measure applications shown in Figure 6. However, a piecewise linear approximation provides a shift of all scaling ranges toward larger values compared with the linearity measure application. The piecewise linear approximation also leads to smaller fractal dimensions in largest scale range than does linearity measure. The grass transects have fairly uniform fractal parameters, whereas the shrub transects appear to have some differences between east-west and north-south transects.

The piecewise linear approximation of the power spectra data resulted in estimates of fractal dimensions that were mostly out of the acceptable range between 1 and 2.

Airborne laser altimetry creates large data sets that may be difficult to visualize and manage. We evaluated three techniques to see if they have any effect on the fractal properties of laser altimetry data: (1) using shorter transects, (2) block averaging, and (3) data decimation.

To assess the effects of using shorter transects on fractal parameters, existing transects were divided into five equal subtransects. The RMS roughness and fractal parameters were calculated at scales that were within 20% of the length of the new transects. We did not find any statistically significant differences between averaged values of parameters obtained for subtransects and the estimates of the same parameters for the parent transect.

Block averaging markedly diminished roughness at low scales (Figs. 6a, 6c, and 6d). Scaling was still possible, but the fractal dimension at low scales was diminished and the range of scaling between 4 and 20 m disappeared (Fig. 7a). Other linearity intervals and values of fractal dimensions in these intervals were preserved.

Reducing the number of points by preserving each fifth or tenth point did not decrease the roughness (Figs.

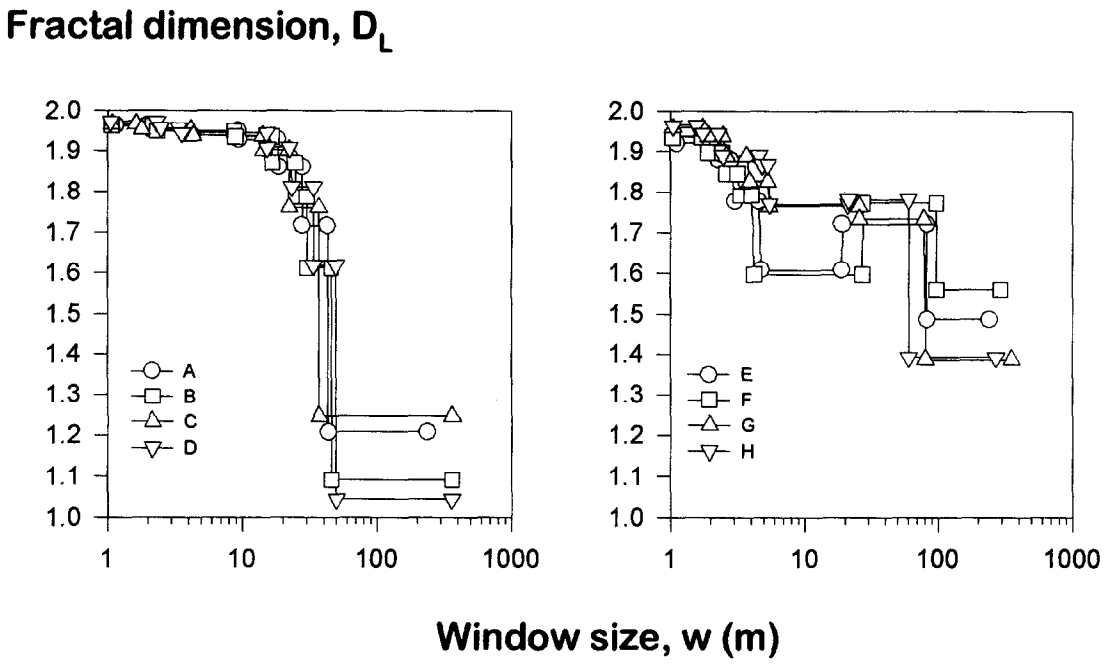

Figure 5. Intervals of linearity and fractal dimensions estimated by applying linearity measure of Yokoya et al. (1989) to dependencies of the root-mean-square roughness on the window size: (A–D) grass transects; (E–H) shrub transects.

7e and 7f). Such reduction, however, leads to smoothing dependencies of the fractal dimension on the scale, as shown in Figure 7b. A moving averaging resulted in both decrease of roughness and smoothing dependencies of the fractal dimension on the scale as shown in Figures 7b and 7c.

DISCUSSION

Fractal scaling appears to be applicable to the data of laser altimetry. However, a hierarchical arrangement of fractals in a scale-dependent model was needed to simulate the irregularity revealed by laser altimetry data.

The graphs of grass and shrub transects showing scale dependent root-mean-square roughness have quite different shapes. The values of roughness at scales of about 1–2 m is the same in all transects. This level of roughness probably manifests the intrinsic irregularity of data caused by random and systematic system noise. Almost the same roughness and the fractal dimension close to 2 exist in grass transects on scales from 1 to 20 m. This probably means that no particular feature of landscape is pronounced within these scales. In shrub transects, scales between 4 and 30 m represent an interval where the roughness is significantly diminished. Scaling in this range may reflect a similarity in dune and shrub

Table 1. Fractal Parameters Obtained by Using a Piecewise Linear Approximation of Log (Roughness)–Log (Window Size) Dependencies for Grass (A, B, C, D) and Shrub (E, F, G, H) Transets

Transect	Roughness over 1-m Windows	Lower Boundaries of the Linearity Ranges (m)			Fractal Dimensions over the Linearity Ranges			
		2[a]	3	4	1	2	3	4
A	0.12	35.1	81.2	nd[b]	1.92	1.44	1.09	nd
B	0.12	29.8	64.7	nd	1.93	1.48	1.07	nd
C	0.12	25.4	45.6	nd	1.93	1.66	1.24	nd
D	0.12	36.2	83.3	nd	1.92	1.40	1.00	nd
E	0.12	4.23	11.5	147.1	1.87	1.63	1.67	1.24
F	0.12	4.62	22.2	134.2	1.87	1.58	1.74	1.46
G	0.12	3.83	59.8	100.1	1.93	1.77	1.58	1.38
H	0.12	4.20	61.7	119.8	1.93	1.79	1.56	1.25

[a] The lower boundary of linearity range 1 is set at 1 m. Because of the piecewise approximation used, range 2 begins where range 1 ends, range 3 begins where range 2 ends, and range 4 begins where range 3 ends.
[b] Not defined.

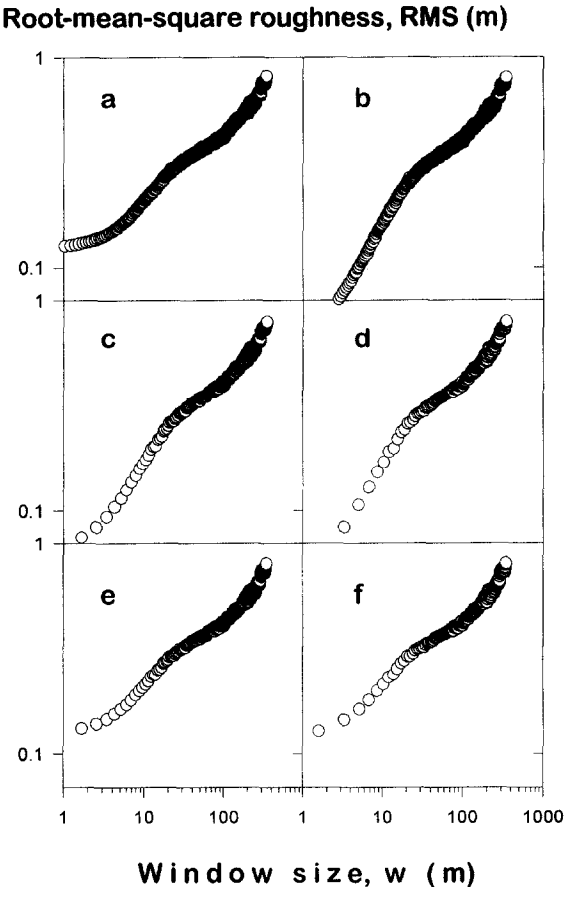

Figure 6. Effect of sampling and resampling on dependencies of root-mean-square roughness on length of intervals over which it was calculated (window size) for the shrub transect: (a) original data set; (b) 7-point moving average in each point; (c, d) block average—5 and 10 points in a block, respectively; (e, f) decimating data—taking each fifth and each tenth point, respectively.

size and placement. The range of scale (6 to 30 m) is also similar to the diameter of dunes along these transects. The difference between scaling for the east-west and north-south transects in Table 1 may be due to dune shape. Because the dunes have their longest diameter in the southwest to northeast direction, the difference in fractal dimensions between the east-west and north-south transects may be due to dune orientation. This anisotropy of the fractal dimension is qualitatively similar to the anisotropy reported by Fox and Hayes (1985) and Loehle (1994) for generated and natural surfaces that are close to plane waves. The next interval of scaling between 30 and 60–90 m may reflect features of both topography and vegetation related to the arrangement of shrubs in clumps. This hypothetical explanation of the existence of several scale ranges corresponds to the observation made by Mark and Aronson (1984) that the limits of self-affinity generally correspond to some typical feature in the landscape.

Scales larger than 60–90 m are probably reflecting self-affine arrangement of the relief. Grass landscapes have lower fractal dimensions in this range of scales. Culling and Datko (1987) have suggested that a general diffusion degradation regime will tend to smooth the landscape and thereby decrease the fractal dimension. On the other hand, they have pointed out that drainage systems will tend to add irregularity to the landscape through incision and rejuvenation and will increase the value of the fractal dimension. We hypothesize that, in the site of our studies, the landscapes with larger fractal dimensions may be more suitable for shrub growth because of the presence of the coppice dunes.

The increase in fractal dimension in shrubs at scales between 30 and 60–90 m in principle could be related to a periodicity in elevation data. We calculated semivariograms of the data (not shown) and did not find any indication of the presence of a periodic component in our data, because all semivariograms were monotonously increasing functions.

Overall, the fractal dimensions and irregularities decreased as the scale increased in this study. The opposite trend was also observed. For example, Polidori et al. (1991) considered two scales and obtained D_s=2.07 for the 1–5 pixel interval and D_s=2.25 for the 10–30 pixel interval. The two distance intervals were chosen to discriminate between distances over which the interpolation process is relevant (the shortest one) and those over which it is not (the largest one). Interpolation is a smoothing operation that diminishes the fractal dimension (Gilbert, 1989). This may explain why the small scale data were less irregular in the study of Polidori et al. (1991).

Applications of the power spectrum method to our data led to results that do not have physical meaning. Other researchers have encountered similar problems (Gilbert, 1989). Large errors associated with this method often occur (Talibuddin and Runt, 1994). Williams and Beebe (1993) compared power spectrum and RMS roughness methods and found the power spectrum method to be inaccurate. Examples used in our paper show that there may be serious restrictions in applicability of the power spectrum method to data with a scale-dependent self-affinity.

Results of the RMS roughness method depend on the selection of intervals of linearity representing ranges of the self-affine fractal scaling on log(roughness)-log (scale) plots. Although both the linearity measure technique and the piecewise linear approximation were acceptable, both techniques have deficiencies. The linear measure technique presumes that a new interval of linearity begins just where the preceding interval ended. This may mask the presence of a curvilinear transition zone between two linear segments. The piecewise linear approximation includes residuals in curvilinear transition zones into the sum of squared residuals that is mini-

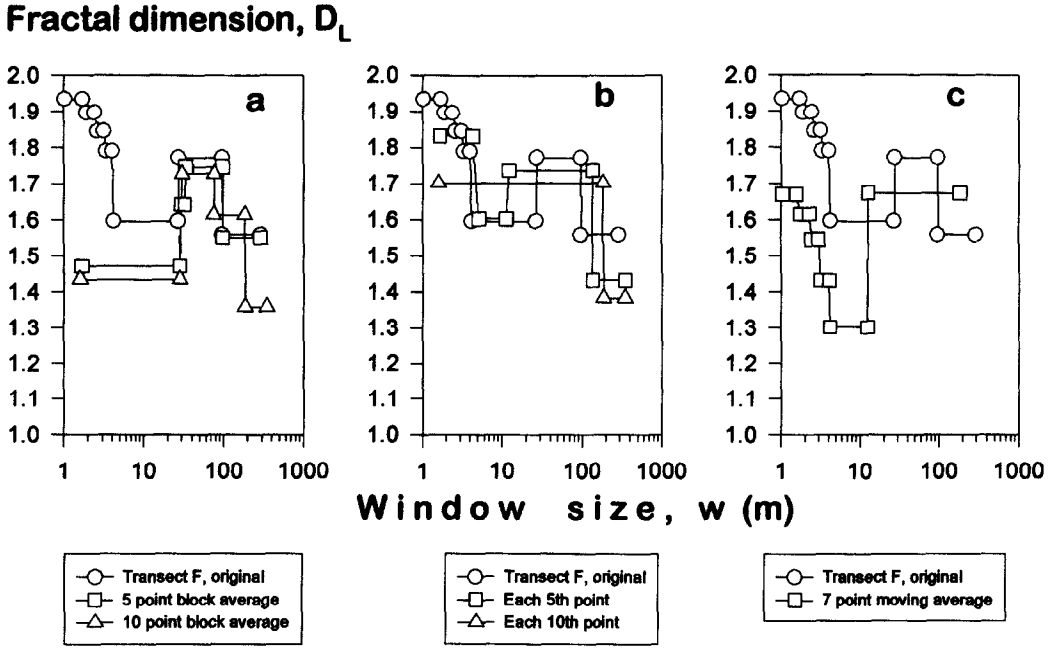

Figure 7. Effect of sampling and resampling on intervals of linearity and fractal dimensions estimated by applying the linearity measure of Yokoya et al. (1989) to data on shrub transect: (a) effect of block averaging; (b) effect of data decimating; (c) effect of moving averaging.

mized. This represents the disadvantage that data on grass transects best illustrate. The middle scale (range 2 in Table 1) defined for those transects is an artifice to keep two linear intervals close to data points. Such an artifice introduces a nonphysical entity and distorts the fractal dimension in the ranges where scaling is applicable. However, a two-piece linear approximation produces unacceptable results without this artifice. More studies are needed on separation of scaling range in multiscale data sets of laser altimetry.

Numerical experiments with data resampling and filtering show that these operations may alter estimates of fractal parameters. Our results are in general agreement with the data of Gilbert (1989), who applied moving average, data decimation, and linear interpolation to sonar data and found decreases in fractal dimensions.

The closeness of parameters obtained from subtransects to the parameters of the parent transect shows that the scaling ranges and parameters are applicable all over the transect and that the same scaling exists all over the transects. The working assumption here is that a subtransect is a representative sample of the parent transect; otherwise fractal dimensions may change.

The data obtained from transects are useful for discovering scaling properties of the landscape roughness. However, much more information about scaling properties and anisotropy of roughness can be extracted from two-dimensional data on the surface elevations (De Jong and Burrough, 1995; Loehle, 1994; Russ, 1994). New equipment allows collection of two-dimensional altimetry data for comparison of one-dimensional and two-dimensional data in discriminating landscapes and in estimating aerodynamic roughness of the land surfaces in these landscapes. The high density of the two-dimensional laser altimetry data would make them suitable for testing new scaling models, with multifractal scaling being the first choice. The presence of multifractal scaling can be tested by considering data at different scales; as the resolution decreases, the structures on multifractal images become smoother and are found to occupy an increasing fraction of images, while simultaneously decreasing in value (dimming) to compensate (Lovejoy and Schertzer, 1991).

The difference between fractal parameters of laser altimetry data for grass and shrub landscapes by supports the possibility of distinguishing between these landscapes by using laser altimetry. Results show that a specific range of scales has to be selected to use the fractal dimension for distinguishing between grass and shrub landscapes. We realize that ranges of the fractal scale dependencies may be specific for our study. It remains to be seen whether several different ranges of fractal scaling of roughness can be found in other landscapes. Calculation of fractal dimensions from log-log plots involves the slope and intercept parameters. Whereas the slope is used directly to calculate the fractal dimension, the intercept is an important measure of the vertical range or amplitude and is another parameter characterizing fractal scaling (Malinverno, 1990). This value defines such parameters of the surface roughness as the crossover length, topothesy, and so forth. This parameter can be included in the distinguishing procedure (Hallet, 1989). It remains

to be seen whether seasonal changes of the vegetation modify or change the scaling laws of the surface roughness. All these questions represent exciting horizons to explore.

The authors express appreciation to the USDA-ARS Remote Sensing Research Unit, Subtropical Agricultural Research Laboratory, Weslaco, TX, for the use of their Aerocommander as the platform for flying the instrument. Special appreciation goes to M. R. Davis, pilot, USDA-ARS, Weslaco, TX, who flew the Aerocommander. Sincere appreciation is due the staffs of the USDA-ARS Jornada Experimental Range, Las Cruces, NM, the USDA-ARS Hydrology Laboratory, Beltsville, MD, and the USDA-ARS Remote Sensing and Modeling Laboratory, Beltsville, MD, who provided logistical and ground support before, during, and after the airborne campaigns. We are grateful to Dr. M. Menenti and Dr. E. Perfect, for their suggestions for improvements in the original manuscript, and to three reviewers who made other helpful suggestions.

REFERENCES

Andrle, R., and Abrahams, A. D. (1990), Fractal techniques and the surface roughness of talus slopes: reply. *Earth Surface Processes Landforms* 15:283–285.

Buffington, L. C., and Herbel, C. H. (1965), Vegetational changes on a semidesert grassland range from 1853 to 1963. *Ecol. Monogr.* 35:139–164.

Carr, J. (1990), Surface roughness characterization of rock masses using the fractal dimension and the variogram. *Technical Report No. REMR-GT-14*, U.S. Army Waterways Experimental Station, Vicksburg, MS.

Culling, W. E. H., and Datko, M. (1987), The fractal geometry of the soil-covered landscape. *Earth Surface Processes and Landforms* 19:369–385.

DeCola, L. (1989), Fractal analysis of a classified Landsat scene. *Photogramm. Eng. Remote Sens.* 55:601–610.

De Jong, S. M., and Burrough, P. A. (1995), A fractal approach to the classification of Mediterranean vegetation types in remotely sensed images. *Photogramm. Eng. Remote Sens.* 61: 1041–1053.

Dubuc, B., Quiniou, J. F., Roques-Carnes, C., Tricot, C., and Zucker, S. W. (1989), Evaluating the fractal dimension of profiles. *Phys. Rev. A* 39:1500–1512.

Fox, C. G., and Hayes, D. E. (1985), Quantitative methods for analyzing the roughness of the seafloor. *Rev. Geophys.* 23:1–48.

Gilbert, L. E. (1989), Are topographic data sets fractal? *Pure Appl. Geophys.* 131:241–254.

Gregotsky, M. E., Jensen, O., and Arkani-Hamed, J. (1991), Fractal stochastic modeling of aeromagnetic data. *Geophysics.* 56:1706–1715.

Hallet, B. (1989), Spatial self organization in geomorphology: from periodic bedforms and patterned grounds to scale-invariant topography. *Earth Sci. Rev.* 29:57–75.

Jaggi, S., Quatrochi, D. A., and Nam, N. S.-N. (1993), Implementation and operation of three fractal measurement algorithms for analysis of remote-sensing data. *Comput. Geosci.* 19:745–767.

Klinkenberg, B., and Goodchild, M. (1992), The fractal properties of topography: a comparison of methods. *Earth Surface Processes Landforms* 17:217–234.

Lam, N. S.-N. (1990), Description and measurement of Landsat TM images using fractals. *Photogramm. Eng. Remote Sens.* 56:187–195.

Loehle, C. (1994), Estimation of fractal dimensions from transect data. Argonne National Laboratory Report No. ANL/ER/PP-74994.

Lovejoy, C., and Schertzer, D. (1990), Multifractals, universality classes, and satellite and radar measurements of cloud and rain fields. *J. Geophys. Res.* 95:2021–2034.

Malinverno, A. (1989), Testing linear models of sea-floor topography. *Pure Appl. Geophys.* 131:139–155.

Malinverno, A. (1990), A simple method to estimate the fractal dimension of a self-affine series. *Geophys. Res. Lett.* 17: 1953–1956.

Mandelbrot, B. (1986), Self-affine fractal sets II: length and surface dimensions. In *Fractals in Physics* (L. Pietronero and E. Tosatti, Eds.), North-Holland, Amsterdam, pp. 3–15.

Mark, D., and Aronson, P. (1984), Scale-dependent fractal dimensions of topographic surfaces: an empirical investigation, with applications on geomorphology and computer mapping. *Math. Geol.* 16:671–683.

Menenti, M., and Ritchie, J. C. (1994), Estimation of effective aerodynamic roughness of Walnut Gulch watershed with laser altimeter measurements. *Water Resour. Res.* 30: 1329–1337.

Ouchi, S., and Matsushita, M. (1992), Measurement of self-affinity on surfaces as a trial application of fractal geometry to landform analysis. *Geomorphology* 5:115–130.

Pachepsky, Y. A., Polubesova, T. A., Hajnos, M., Jozefaciuk, G., and Sokolowska, Z. (1995), Fractal parameters of pore surface area as influenced by simulated soil degradation, *Soil Sci. Soc. Am. J.* 59:68–75.

Pfeifer, P., and Obert, M. (1990), Fractals: basic concepts and terminology. In *The Fractal Approach to Heterogeneous Chemistry* (D. Avnir, Ed.), Wiley, New York, pp. 11–43.

Polidori, L., Chorowicz, J. and Guillande, R. (1991), Description of the property of self-similarity is called self-affinity for vertical terrain as a fractal surface, and application to digital elevation profiles or for terrain surface itself: model quality assessment. *Photogramm. Eng. Remote Sens.* 57:1329–1332.

Press, W. T., Teukolsky, S. A., Vettering, W. T., and Lannery, B. P. (1990), *Numerical Recipes: The Art of Scientific Computing*. Cambridge University Press, New York.

Rees, D., and Miller, J.-P. (1990), Surface roughness estimation using fractal variogram analysis. In *Proceedings of the International Geoscience and Remote Sensing Symposium (IGARSS '90)*. pp. 1951–1954, 20–24 May, College Park, MD.

Ritchie, J.C. (1995), Airborne laser measurements of landscape topography. *Remote Sens. Environ.* 53:91–96.

Roach, D. E., and Fowler, A. D. (1993), Dimensionality analysis of patterns: fractal measurements. *Comput. and Geosci.* 19:849–869.

Russ, J. C. (1994), *Fractal Surfaces*, Plenum Press, New York.

Shepard, M.K., Brackett, R. A., and Arvidson, R. E. (1995), Self-affine (fractal) topography: surface parameterization and radar scattering. *J. Geophys. Res.* 100:11,709-11,718.

Talibuddin, S., and Runt, J. P. (1994), Reliability test of popu-

lar fractal techniques applied to small two-dimensional self-affine data sets. *J. Appl. Phys.* 76:5070–5078.

Turcotte, D. L. (1992), *Fractals and Chaos in Geology and Geophysics*. Cambridge University Press, Cambridge, UK.

Whitmore, A. P. (1991), A method for assessing the goodness of computer simulation of soil processes. *J. Soil Sci.* 42:289–299.

Williams, J. M., and Beebe, T. R. Jr. (1993), Analysis of fractal surfaces using scanning probe microscopy and multiple image variography 2: results on fractal and non-fractal surfaces, observation of fractal crossovers, and comparison with other fractal techniques. *J. Phys. Chem.* 97:6255–6260.

Yokoya, N., Yamamoto, K., and Funakuro, N. (1989), Fractal-based analysis and interpolation of 3D natural surface shapes and their application to terrain modeling. *Comput. Vision Graphics Image Process.* 46:284–302.